Chapter 2
Rapid Mapping Using Airborne and Satellite SAR Images

Fabio Dell'Acqua and Paolo Gamba

2.1 Introduction

Historically, Synthetic Aperture Radar (SAR) data was made available later than optical data for the purpose of land cover classification (Landsat Legacy Project Website, http://library01.gsfc.nasa.gov/landsat/; NASA Jet Propulsion Laboratory: Missions, http://jpl.nasa.gov/missions/missiondetails.cfm?mission=Seasat); in more recent times, the milestone of spaceborne meter resolution was reached by multispectral optical data first (Ikonos; GEOEye Imagery Sources, http://www.geoeye.com/CorpSite/products/imagery-sources/Default.aspx#ikonos), followed a few years later by radar data (COSMO/SkyMed [Caltagirone et al. 2001] and TerraSAR-X [Werninghaus et al. 2004]). As a consequence, more experience has been accumulated on the extraction of cartographic features from optical rather than SAR data, although in some cases radar data is highly recommendable because of frequent cloud cover (Attema et al. 1998) or because the information of interest is better visible at the microwave frequencies rather than at the optical ones (Kurosu et al. 1995).

Unfortunately, though, SAR data cannot provide complete scene information because radar systems operate on a single band of acquisition, a limitation which is partly compensated, and only in specific cases, by their increasingly available polarimetric capabilities (Treitz et al. 1996).

Nonetheless, the launch of new generation, Very High Resolution (VHR) SAR satellites, with the consequent perspective availability of repeated acquisitions over the entire Earth, do push towards the definition of novel methodologies for exploiting these data even for extraction of cartographic features. This does not mean that a replacement is in progress over the traditional way of cartographic mapping, based on airborne and, more recently, spaceborne sensors in the optical and near infrared regions. There is instead the possibility for VHR SAR to provide basic and complementary information.

F. Dell'Acqua (✉) and P. Gamba
Department of Electronics, University of Pavia. Via Ferrata, 1 - I-27100 Pavia
e-mail: fabio.dellacqua@unipv.it; paolo.gamba@unipv.it

U. Soergel (ed.), *Radar Remote Sensing of Urban Areas*, Remote Sensing and Digital Image Processing 15, DOI 10.1007/978-90-481-3751-0_2,

It has been indeed proven that SAR data is capable of identifying some of the features reputed to be among the most complex to be detected in remotely sensed images (e.g. buildings, bridges, ships, and other complex-shaped objects); semi-automatic procedures are already available providing outputs at a commercially acceptable level. Some examples include the definition of urban extent (He et al. 2006), discrimination of water bodies (Hall et al. 2005), vegetation monitoring (Askne et al. 2003), road element extraction (Lisini et al. 2006), entire road network depiction (Bentabet et al. 2003), and so on. Moreover, the interferometric capabilities of SAR, where available, allow the exploitation of terrain and object height to improve the cartographic mapping process (Gamba and Houshmand 1999).

In terms of cost and possibility of covering large areas, SAR is indeed widely exploited for three-dimensional characterization of the landscape. This can be used to characterize road networks (Gamba and Houshmand 1999), buildings (Stilla et al. 2003) and, more generally, to discriminate between different kinds of cartographic features.

The main obstacle on the way of these processes towards real-world, commercial applications is probably their specialisation on just one among the possible features of cartographic interest. Although a number of approaches intended for SAR image analysis have appeared in technical literature, no single one is expected to cover all the spatial and spectral features needed for a complete process of cartographic feature extraction starting from scratch.

Road extraction, for instance, is treated in many papers (Mena 2003), but this is seldom connected to urban area extraction and the use of different strategies according to the urban or non-urban areas (see Tupin et al. 2002 or Wessel 2004). The same holds for the reverse approach.

In the following it will be shown an example of how an effective procedure can be assembled starting from some of the above cited or similar algorithms, and thus exploiting as much as possible the full range of information available in a SAR scene acquired at high spatial resolution.

The final goal of the research in progress is a comprehensive approach to SAR scene characterization, attentive to the multiple elements in the same scene. It is thus based on multiple feature extraction and various combination/fusion algorithms. Through an analysis of many different details of the scene, either spectral or spatial, a quick yet sufficiently accurate interpretation of a SAR scene can be obtained, useful for focusing further extraction work or as a first step in more precise feature extraction steps.

The stress in this chapter is placed onto the so-called "rapid mapping" which summarizes the above concept: a fast procedure to collect basic information on the contents of a SAR scene, useful in those cases where the limited amount of information needed does not justify the use of complex, computationally heavy procedures or algorithms.

2.2 An Example Procedure

We illustrate the concept of rapid mapping and the choices and technical solutions behind it by making reference to a procedure proposed by the authors of this chapter, and described more in detail in (Dell'Acqua et al. 2008).

In most cases scene interpretation starts from a segmentation of the image based on some sort of knowledge embedded into the algorithms and then proceeds to analyse each single segment more in detail, possibly further partitioning it. The reference procedure also uses this approach which is commonly termed "top-down", meaning that the interpretation starts from the "top" level objects (biggest objects, largest partitions, widest categories) successively moving "down" (to smaller objects, . . .) better specifying and possibly also perfecting the recognition and analysis of the objects found. The procedure in (Dell'Acqua et al. 2008) features also contemporary exploitation of spatial (texture analysis, extraction and combination of linear elements) and radiometric (mostly local intensity) features.

The general information flow is visible in Fig. 2.1, while the proposed standard structure is presented in Fig. 2.2. The next subchapters describe how the basic information can be extracted from a given high-resolution SAR image.

2.2.1 Pre-processing of the SAR Images

The example procedure, as shown in Fig. 2.2, is performed stepwise starting from the easiest-to-extract land cover moving on to categories requiring more complicated processing or obtainable by exclusion of the former –already assigned- land covers. It is worthwhile mentioning that the entire procedure can be realized relying also on other algorithms than those cited in the present chapter, provided that those can guarantee a comparable accuracy and quality of results. The procedure is not particularly demanding in terms of the data characteristics: input data are single-polarisation, single-date amplitude images. Results may benefit from fusion with multi-polarisation and/or multitemporal data; research is underway to fuse information coming from more images or more polarisation, but results are not yet assessed and not worthwhile being presented here.

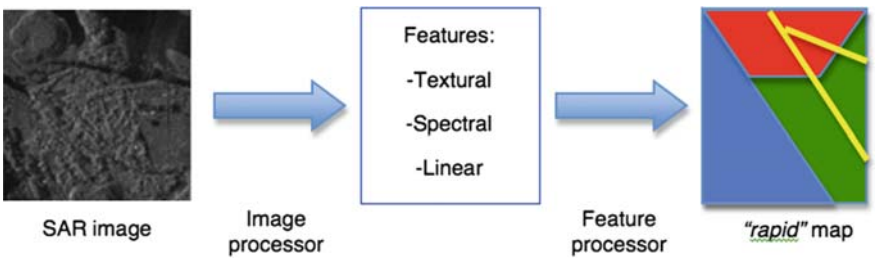

Fig. 2.1 The information flow

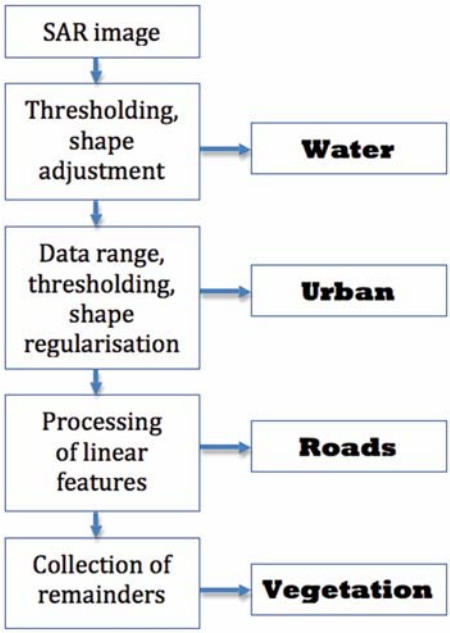

Fig. 2.2 Processing steps

One of the first steps is speckle removal, which is in general useful but has shown to be not really indispensable for rapid mapping. Probably thanks to the extraction of geometric features, which is nearly independent from the single pixel value, experiments have shown indeed that even when the speckle-filtering step is completely skipped, the worsening in the quality of final results is not significant. In our experiments we have used the classical Lee filter and performed filtering on all the images, as the tiny saving in computation time does not justify working on unfiltered images.

Let us now consider the various land cover/element extraction steps in the respective order: water bodies, human settlements, road network, vegetated areas.

2.2.2 Extraction of Water Bodies

It is commonly acknowledged that internal water bodies are one of the easiest land covers to detect in SAR images, as calm water surfaces cause mirror-like reflection to reflect the incident electromagnetic wave away from the sensor. This results in a particularly low backscatter (Hess et al. 1990; Horritt et al. 2003) which in turn–thanks to the noise being multiplicative- translates into a homogeneous, nearly featureless and textureless (Ulaby et al. 1986) region in the water-covered area in a SAR image.

Moreover, inner water bodies cover areas several pixel wide and form shapes which can be considered smooth and regular even at high spatial resolution. Therefore a thresholding of the image can be used and followed by a procedure like the one described in (Gamba et al. 2007). There, the reasoning behind regularization is applied to building, but the same considerations may be easily found to be applicable also to water bodies. The procedure is split into two steps, the first one devoted to better delineate edges and separate elements, while the second step aims instead at filling possible small holes and gaps inside an object, generally resulting from local classification errors. The reader is referred to (Gamba et al. 2007) for more details on the procedure. Alternative procedures for regularisation may be considered such as (Heremans et al. 2005), based on an adjustment of a procedure (Chesnaud et al. 1999) conceived for general object extraction in images. As mentioned in the introduction, it is not crucial to choose one or the other method for extraction of the single object as far as a reasonable accuracy can be achieved, even more so with easy-to-extract water bodies.

2.2.3 Extraction of Human Settlements

Several methods have been proposed so far for detecting human settlements in radar remotely sensed images, most of them being efficient in detecting the sheer presence of human settlements but generally showing poor performances in precisely delineating the extent of the urban areas (Gouinaud and Tupin 1996). Methods relying on a priori knowledge (Yu et al. 1999) to improve classification are not usable for rapid mapping purposes and one should rather attempt to make the extraction more precise by exploiting textural information (Duskunovic et al. 2000; Dekker 2003; Dell'Acqua and Gamba 2003) and even spatial proximity information based, for example, on Markov Random Fields (Tison et al. 2004). An important issue is however the scale of the texture considered, and this is becoming especially relevant with the increasing availability of VHR SAR images. Such issue is discussed in (Dell'acqua et al. 2006), where an approach combining co-occurrence matrix and semivariogram analysis was tested for mapping urban density in satellite SAR data. Results show that, in terms of final classification accuracy, the joint use of those two features to optimize the texture window size can be nearly as effective as an exhaustive search. A methodology is thus introduced to compute the co-occurrence features with a window consistent with the local scale, provided by the semivariogram analysis. Orientation is the second important issue after scale, and for a discussion of texture orientation the reader is referred to (Pesaresi et al. 2007) where optical images are considered but some geometric considerations may be extended to SAR images as well.

We will illustrate here the approach proposed in (Dell'Acqua et al. 2008) which relies on a simple, isotropic occurrence measure, namely data range or the difference between the maximum and the minimum pixel intensity value in the considered local window. Three steps compose the procedure.

In the first step a pre-scaling of the image to a pixel size of 5 m is performed, according to the considerations expressed in (Pesaresi et al. 2007), and a 5×5 pixel window is used to compute data range, resulting in a $25 \times 25\ m^2$ area to be analysed for the local texture measure computation.

The second step consists of a threshold operation over the computed occurrence map. The threshold value is generally determined heuristically, and a value of 100 was found to provide acceptable results in most cases after a radiometric rescaling of the texture image values to the range 0–255 has been performed. Criteria for a suitable, automatic choice of the threshold value are under investigation. This step is the one where previously performed speckle filtering can make some difference to the accuracy of the results, although the next step is intended also to suppress pixel-wise errors due to local speckle peaks.

The third and last step consists of spatial homogenisation in the form of morphological closing. Again, based on the considerations in (Pesaresi et al. 2007), a size of 5×5 pixels has been used for the morphological operator, which is applied twice as in our experience this produces better results. More refined techniques can be found in (Soille and Pesaresi 2002); however, a reasonable balance between accuracy and complexity should be made before using more sophisticated algorithms where rapid mapping is the context at hand.

A typical, critical pattern for the algorithm outlined above consists of tall trees when they are sufficiently sparse to cause isolated reflection peaks. Some improvement can however be obtained by exploiting relationship with formerly extracted water bodies: it is quite uncommon to find small clusters of urban pixels at a 5 m scale aside a water body, and a buffer area around this latter can be cleared of all urban area pixels as assigned by the texture thresholding step. A further refinement may rely on the exclusion of strongly textured areas, which are likely to be caused by sparse trees, although this implies computation of other texture measures and thus a heavier computational burden. An active research line in this direction is to exploit local extraction of linear features in very high-resolution images to better distinguish urban areas, characterised by man-made features, which are expected to contain several straight lines visible in the images (Aldrighi et al. 2009).

2.2.4 Extraction of the Road Network

The next step consists of extracting another very important piece of information for mapping purposes, that is the main road network. In order to differentiate the problem between two very different contexts, the road network is extracted in non-urban areas first and then within urban areas.

In non-urban areas, that is outside the areas which have been assigned to the "urban" class in the previous steps, a trivial simplification consists of discarding all the areas recognised as belonging to other extracted land-cover classes, that is water and tall trees. In the remaining area, many approaches can be used for road extraction. This problem has been indeed considered for quite a long time

(Bajcsy and Tavakoli 1976) and many different algorithms have been proposed over the years. Naturally, at an initial stage the work concentrated on aerial, optical images. Fischler et al. (1981) used two types of detectors: one optimised against false alarms, and another optimised against misdetections, and combined their responses using dynamic programming. McKeown and Denlinger (McKeown and Denlinger 1988) proposed a road-tracking algorithm for aerial images, which relied on road-texture correlation and road-edge following.

At the time when satellite SAR images started becoming widely available, methods focussed on this type of data made an appearance. Due to the initially coarse resolution of the images, most of such methods exploit a local criterion evaluating radiometric values on some small neighbourhood of a target pixel to start discriminating lines from background, possibly relying on classical edge extractors such as Canny (1986). These segments are eventually connected into a network by introducing larger-scale knowledge about the structures to be detected (Fischler et al. 1981). In an attempt to generalise the approach (Chanussot et al. 1999) extracted roads by combining results from different edge detectors in a fuzzy framework.

Noticeably these approaches refer to the geometrical or structural context of a road, undervaluing its radiometric properties as a region. These are instead considered in Dell'Acqua and Gamba (2001) and Dell'Acqua et al. (2002), where the authors propose clustering of pixels that a classifier has assigned to the "road" class. In the cited papers the authors try and discriminate roads by grouping "road" pixels into linear or curvilinear segments using modified Hough transforms or dynamic programming. The dual approach is proposed in (Borghys et al. 2000), where segmentation is used to skip uniform areas and concentrate the extraction of edges where statistical homogeneity is lower.

Tupin et al. (1998), proposed an automatic extraction methodology for the main axes of road networks. They presented two local line detectors and a method for fusing the information obtained from these detectors to obtain segments. The real roads were identified among the segment candidates by defining a Markov random field for the set of segments. Jeon et al. (1999), proposed an automatic road detection algorithm for radar satellite images. They presented a map-based method based on a coarse-to-fine, two-step matching process. The roads were finally detected by applying snakes to the potential field, which was constructed by considering the characteristics and the structures of roads. As opposed to simple straight-line element detection, in (Jeon et al. 2002), the authors propose extraction of curvilinear structures associated to the use of a genetic algorithm to select and group best candidates in the attempt to optimise the overall accuracy of the extracted road network.

With the increasing availability of new generation, very-high-resolution spaceborne SAR data, multiresolution approach are becoming a sensible choice. In (Lisini et al. 2006), the authors propose a method for road network detection from high-resolution SAR data that includes a data fusion procedure in a multiresolution framework. It takes into account the information available by both a line detector and a classification algorithm to improve the road segment selection and the road network reconstruction. This could be used as a support for rapid mapping over HR spaceborne SAR images.

To complement road extraction in rural areas, extraction of urban road network is the next step. In this environment the scale of relevant objects is much smaller and thus the meter-resolution becomes a requirement. Since in VHR SAR images the roads no longer appear as single image edges but rather as dark, elongated areas with side edges generally brighter than the inside, the strategy needs to be slightly changed. Therefore, one may detect roads by searching pairs of parallel edges or dark, elongated, homogeneous areas. What appears to be a promising approach is fusion of results from different detectors, optimised for the different geometric and radiometric characteristics of the road elements, as proposed in (Dell'Acqua et al. 2003).

After the road elements have been detected, a multiscale-feature fusion framework followed by a final alignment (Dell'Acqua et al. 2005), can be made to follow in order to remove false positives and discard repeated, slightly different detection of the same road element.

Finally, if the focus is placed on the extraction of the road network rather than single roads, geometric features contained in the scene (such as junctions, as shown in Negri et al. (2006)) can be used to infer the presence of missed roads and try and complete the extracted road network.

As shown in (Dell'Acqua et al. 2008), a further refinement of the results is possible when SAR and InSAR data are jointly available, this latter producing a DSM (Digital Surface Model) of the observed area. A simple 2-dimensional low-pass filtering of the DSM is used to approximate a DTM (Digital Terrain Model). This allows identifying as buildings the clusters of pixels stemming above the estimated local ground level. The complementary pixel set are potentially parks, places, playgrounds or similar, and roads (urban environment is implied). The first categories can be discriminated thanks to their aspect ratio, expected to be very different with respect to roads. The remaining ground-level pixels are likely to be road pixels, and they may be reused as clues for better road recognition in a fusion process with the initially extracted road network.

2.2.5 Extraction of Vegetated Areas

Assuming that only the limited set of classes mentioned at the beginning is to be discriminated (water, human settlements, roads vegetation) for "rapid mapping" to be performed, once all the other classes have been extracted, the remaining pixels should belong to the vegetation class. Within vegetation it seems quite sensible to try and distinguish trees and woods from low-rise vegetation.

Two approaches are possible to such discrimination, and integration of the results from both approaches seems even more promising (Dell'Acqua et al. 2008). The first approach relies on texture information: woods show a remarkably evident texture, not found in most of the other vegetated land covers. In particular, the co-occurrence measure "correlation" is the best option for discriminating woods and other taller

cultures from the background, since this measure shows significantly larger values on big windows (30×30 m was used in our experiments) and long displacements (around 10 m).

The second approach involves availability and use of 3D data: a difference operation between the DSM and the DTM will highlight the areas where vegetation is present. Please recall the underlying assumption that urban areas have already been detected and thus removed from the areas considered for vegetation detection; buildings, which may generate similar signatures in the DSM-DTM difference, should have already been masked away at this stage.

Even better results can be achieved by combining results from both approaches. A logical AND operation between the two results has been found by experiment to be advantageous in terms of reduction in false positives vs. increase in missed woods.

2.2.6 Other Scene Elements

As a final remark, we may note that a limited amount of further processing may lead to detection and location of further scene elements not directly addressed in the previous subchapters. Examples are represented by intersections between roads and water bodies, which can be identified as bridges with a good degree of confidence (actually, to a combinations of the degree of confidence with which each supporting element was detected); or lake islands, that is vegetated areas completely surrounded by a "water" region. This issue is not however discussed in depth here as the focus of this chapter is on the extraction of information from the SAR image itself rather than on further stages of processing which may lead to the determination of derived pieces of information.

2.3 Examples on Real Data

To illustrate the usefulness of rapid mapping we will refer to a typical application, that is mapping in the context of disaster management, currently performed by institutions like the International Charter on Space and Major Disasters, SERTIT, UNOOSA and others with methods which imply a massive amount of labour by human experts; the procedures may benefit from the support of tailored tools enlarging the fraction of operations required to produce disaster maps. The Sichuan, China earthquake happened on the 12th of May, 2008, and the extensive rescue operations following this tragic event, proved the value of high-resolution optical and radar remote sensing during the emergency response. While optical data provide a fast and simple way to value "at glance" the damage level, radar sensors have showcased their ability to deliver images independent of weather conditions –which were quite poor at that time in the stricken area- and of time of the day, and demonstrated

that in principle they can represent a mean to obtain an up-to-date situation map in the immediate aftermath of an event, which is precious information for intervention planning.

Immediately after the Sichuan earthquake our group did activate immediately two mechanisms to collect data:

- The Italian Civil Protection Department (Dipartimento della Protezione Civile or DPC) was activated to bring help and support to the stricken population; in this framework the European Centre for Training and Research in Earthquake Engineering (EUCENTRE), a foundation of the University of Pavia, as an "expert centre" of DPC was enabled to access COSMO/SkyMed (C/S) data acquired over the affected area
- Our research group is entitled to apply for TerraSAR-X (TSX) data for scientific use following the acceptance of a project proposal connected to urban area mapping submitted in response to a DLR AO

Both the C/S and TSX data covered quite large areas, on the order of ten times 10 km. In order to limit the processing times and avoid dispersing the analysis efforts, the images were cropped to selected subareas. Since the focus of this work is on mapping of significant element rather than damage mapping, in the following we will concentrate only on areas, which reported slight damage or no damage at all, namely:

– C/S sub-image: a village located on the outskirts of Chengdu, around 30°33′ 17.14″N, 104°14′0.18″E; in this area almost no damage was reported. An urban area including a number of wide, well-visible main urban roads aligned to two principal, perpendicular directions, almost no secondary roads. The urban area is surrounded by countryside with low-rise vegetation crossed by a few rural, connecting roads.
– TSX sub-image: Luojiang, no damage, some water surface (TSX) 31°18′27.85″N, 104°29′46.73″E; in this area no damage was reported. The image contains the urban area of Luojiang, crossed by a large river, a big pond, and several urban roads with sparse directions.

These two areas, which reported almost no damage, were chosen to illustrate an application related to disaster mapping, that is "peacetime" extraction of fresh information aimed at keeping maps of the disaster-prone area constantly up-to-date. Other areas of the same images were instead used for damage mapping purposes (Dell'Acqua et al. 2009).

2.3.1 The Chengdu Case

As mentioned above, this urban area was chosen because of its large number of urban roads and indeed the rapid mapping procedure focussed on road extraction. The original COSMO/SkyMed image crop is shown in Fig. 2.3, courtesy of the Italian Space Agency and the Italian Civil Protection Department.

Fig. 2.3 COSMO/SkyMed image of Chengdu outskirts. Italian Space Agency

Fig. 2.4 The urban area extraction procedure

After despeckle filtering, the first processing step performed on this image was extraction of the urban area as described in (Dell'Acqua et al. 2008) and briefly outlined in the scheme in Fig. 2.4. Extraction results appear as a red overlay on the original SAR image in Fig. 2.5.

Looking carefully at the image one can note some facts:

– Some small blocks not connected with the main urban area are missed; note the cluster of buildings located at mid height on the far left side of the image. Although it is quite difficult to tell exactly the reason why the co-occurrence measure ended below the fixed threshold, a reasonable guess is the peculiar shape of the building results in smooth transition between double bounce and mirror reflection areas. This translates into a data range measure lower than commonly found in areas containing buildings.
– Remarkably, where urban areas are detected, their contours are defined accurately. Please refer to the bottom central area of Fig. 2.5, where the irregular boundaries of the urban area are followed with a good correctness.
– Thanks to the morphological closing operation, single buildings are not considered, although they locally cause an above-threshold value for the data range texture measure. An example is the strong reflector located on top centre of the

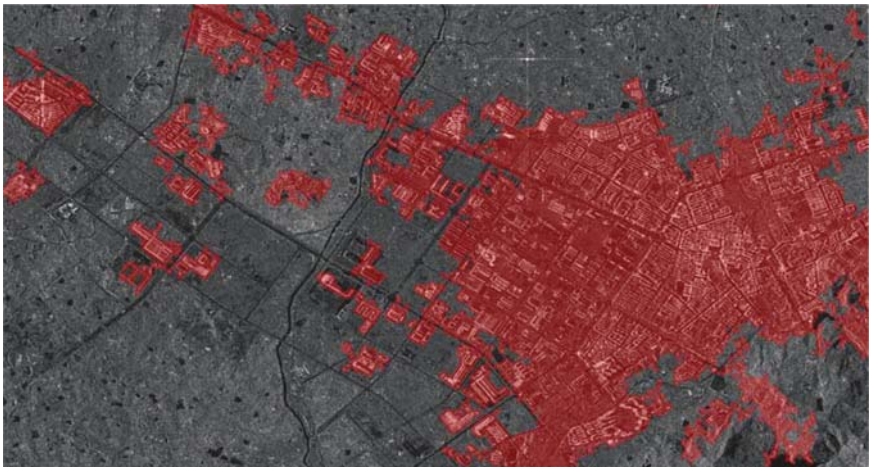

Fig. 2.5 The results of urban area extraction over Chengdu image

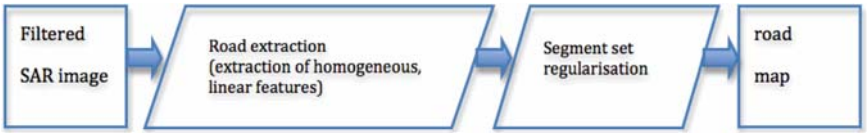

Fig. 2.6 The road extraction procedure

image, which causes the impulse response of the system to appear in the shape of a cross. By inspection of the Google Earth © image of the area, this appears to be a single building probably with a solid metal structure.

The next operation was extraction of the road network (Fig. 2.6), whose results are illustrated in Fig. 2.7. Again, this operation was performed following the procedure described in (Dell'Acqua et al. 2008), and briefly recalled in Fig. 2.6. The urban road system is basically extracted, no important roadway was missed; nonetheless some gaps are visible in a number of roads. The advantage in the context of rapid mapping is that the basic structure of the road network becomes available, including pieces of non linear roads, like for the bend in mid centre left of the image. On the other hand, though, in some cases narrow waterways like the trench flowing vertically across the image are detected as roads. Moreover, the gaps in detected roads prevent the use of the current version of the extractor in an emergency situation where a fast detection of uninterrupted communication lines is required. Nonetheless, the imposition of geometric constraints may be the correct step for completing the road network and keeping maps up-to date.

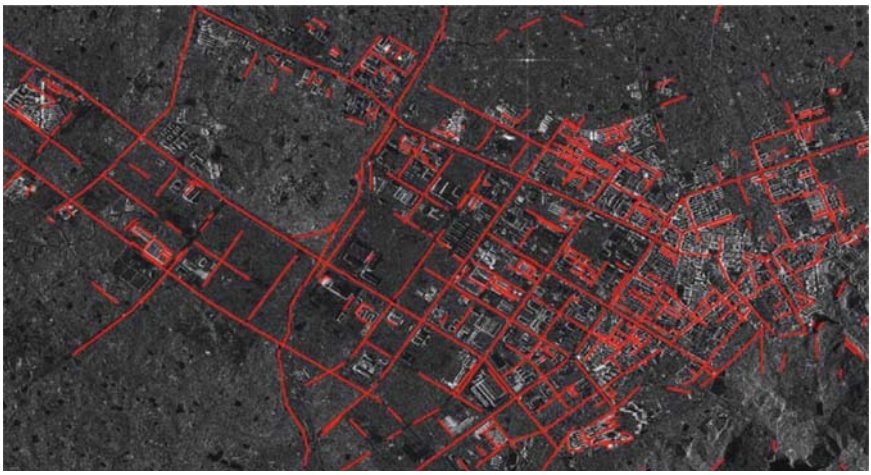

Fig. 2.7 Street network extracted from Chengdu image

2.3.2 The Luojiang Case

The second area selected for experimenting a rapid mapping procedure is the town of Luojiang, featuring less ordered urban roads, a large river crossed by a series of bridges, and two big ponds on top right. The built-up area is actually quite sparse, with clusters of buildings interspersed among bare areas. The corresponding crop of TerraSAR-X image (courtesy of DLR) is shown in Fig. 2.8.

The same procedure (Dell'Acqua et al. 2008) used for the COSMO/SkyMed image was re-applied to this image, and the results of the urban area extraction are shown in Fig. 2.10, left, as a red overlay on the gray-scale SAR image.

Noticeably, the classified urban area correctly reproduces the sparse pattern of blocks in the town, especially in the southernmost area (the images are geo-coded north upwards). Unfortunately, though, some missed buildings are reported in the eastern part of the image, probably due to the lower contrast found in that area.

In Fig. 2.10, left, a blue area represents the result of extracting water bodies in the same image according to the procedure reported in (Dell'Acqua et al. 2008) and briefly recalled in the scheme in Fig. 2.9. Generally speaking, water bodies are extracted conservatively, and several water pixels are missed. No false positives are reported, and a portion of the lower pond in upper right part of the image was lost. This is a consequence of a particularly strict selection of parameters for the extraction of water pixels, favouring correctness against completeness. Different selections of parameters may result in a more balanced situation between correctness and completeness, however discussing this issue is off the scope of this chapter. As a general consideration, the most appropriate strategy will depend on the purpose of the rapid mapping operation; for example, in the case of a flood where non-submerged pieces of land are sought to move people to a temporary haven,

Fig. 2.8 TerraSAR-X image of Luojiang, Sichuan, China

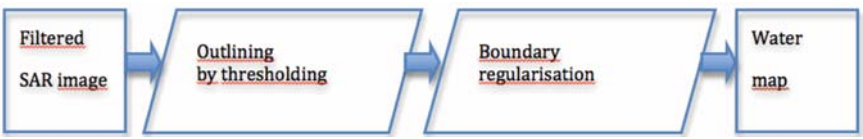

Fig. 2.9 Water land cover extraction procedure

completeness of class should be favoured (fewer pixels reliably classified as land rather than more and unsure), while in case of possible obstruction of a river due to a landslide, correctness is preferable.

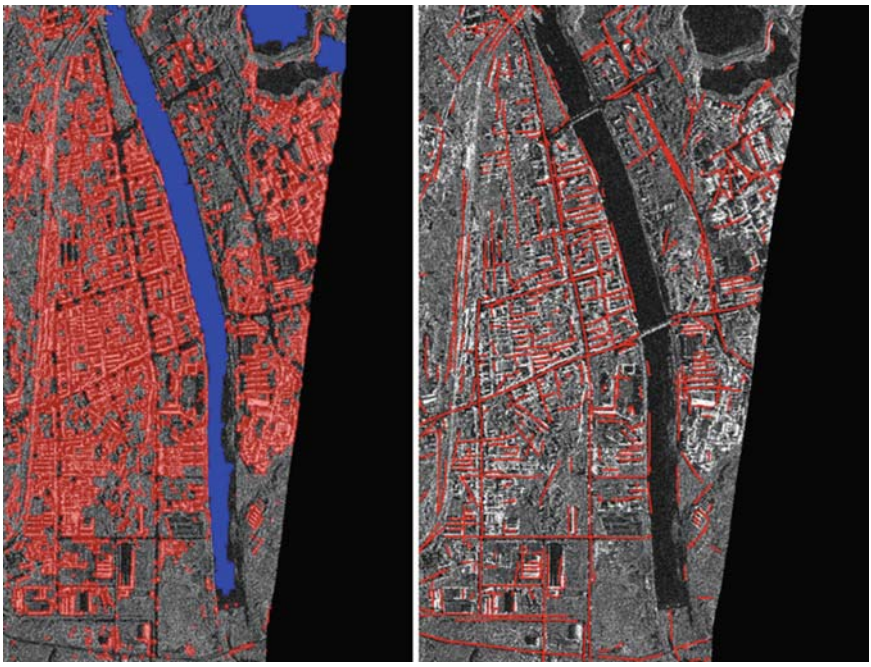

Fig. 2.10 *Left*: Water and urban area extraction; *Right*: Road network extraction on the Luojiang image

Figure 2.10, right, shows the results of road extraction applied to the Luojiang image. As can be seen in the figure, the extracted road network, overlaid in red over the gray-scale image, is quite complete. Just like for the C/S image, boundaries of waterways (in this case, the river) may be confused for roads, but their suppression is achievable by comparison with the water body map. In this sense the extraction of pieces of information from the image can improve the correctness of the following extraction steps, as mentioned in Section 2.2.

Again, a certain number of gaps are reported in the road network, although the overall structure is quite evident from the extraction result. Similar considerations to those made in the previous subchapter apply also to this extraction.

A final step may consist, as anticipated in Section 2.2, of vegetation extraction.

The easiest way to perform such extraction, considering the limited set of land cover classes assumed, is to define vegetation as the remainder of the image once all the other land cover classes have been extracted. Although quite simple, this approach provides acceptable results in a context of rapid mapping, shown for this case in Fig. 2.11, where the "vegetation" class is overlaid to the original gray-scale image. Naturally the accuracy of this result is tied to the accuracy of the former class extraction; if one looks at the missed part of the pond on upper right, it is easy to see that it ended up in the class "vegetation" causing a lower correctness value.

Fig. 2.11 Vegetation extraction over Luojiang image

2.4 Conclusions

The appearance on the scene of the new generation of SAR satellites capable of providing meter and sub-meter resolution SAR scenes potentially over any portion of the Earth surface has overcome the traditional limits connected with airborne acquisition and has boosted research on this alternative source of information in the context of mapping procedures.

Both 2D and, where available, 3D information may profitably be exploited for the so-called "rapid mapping" procedure, that is a fast procedure to collect basic information on the contents of a SAR scene, useful in those cases where the limited amount of information needed does not justify the use of complex, computationally heavy procedures or algorithms.

It has been shown by examples that rapid mapping on HR SAR scenes is feasible once suitable, efficient tools for the extraction of relevant features are available.

Although the proposed results are acceptable for rapid mapping, the usual cartographic applications need accuracy levels that are not achievable with the proposed tools. The two problems are then to be considered as separate items:

- On the one side, "rapid mapping" with its requirement of light computational load and speed in production of results
- On the other side, traditional cartographic applications with much loosed speed requirements but far stricter accuracy constraints

Needless to say, rapid mapping can still be useful to provide a starting point, over which precise cartographic extraction can successively build, in a two-stage approach which is expected to be overall more efficient than addressing directly the precise extraction.

A big advantage of using SAR data for rapid mapping is the availability of 3D interferometric data derived directly through suitable processing of different satellite passes over the site; 3D data is naturally perfectly registered with the underlying 2D radiometric data.

This chapter has presented a general framework for performing rapid mapping based on SAR scenes, but some issues still remain open and deserve further investigation:

- Small clusters of buildings sometimes may not be detected as urban areas and result in the production of false positives for the class "wood".
- The model for roads is a series of linear segments, thus curvilinear roads have to be piecewise approximated, with a consequent loss of accuracy and possibly also completeness. This is a problem especially in higher relief areas where bends are frequent. A curvilinear model for roads should be integrated into the extraction algorithm if this is to be really complete. The trade-off between precision and speed of execution should not however be forgotten.

It is the opinion of the authors that a structure like the one presented in this chapter is a good starting point for the setting up of a "scene interpreter" in a context of rapid mapping over SAR images. The modular structure allows the inclusion of new portions of code or algorithms as needed. Thanks to the increasing availability of very high-resolution spaceborne SAR all over the world, and the capability of those systems to acquire images over a given area within a few days or even hours, will make the topic of rapid mapping to increase its appeal for many applications, especially for those related to disaster monitoring.

Acknowledgements The authors wish to acknowledge the Italian Space Agency and the Italian Civil Protection Department for providing the COSMO/SkyMed image used in the examples of rapid mapping, the German Space Agency (DLR) for providing the TerraSAR-X image, and Dr. Gianni Lisini for performing the processing steps discussed in this chapter.

References

Aldrighi M, Dell'Acqua F, Lisini G (2009) Tile mapping of urban area extent in VHR SAR images. In: Proceedings of the 5th IEEE/ISPRS joint event on remote sensing over urban areas, Shanghai, China, 20–22 May 2009

Askne J, Santoro M, Smith G, Fransson JES (2003) Multitemporal repeat-pass SAR interferometry of boreal forests. IEEE Trans Geosci Remote Sens 41(7):1540–1550

Attema EPW, Duchossois G, Kohlhammer, G (1998) ERS-1/2 SAR land applications: overview and main results. In: Proceedings of IGARSS'08, vol 4, pp 1796–1798

Bajcsy R, Tavakoli M (September 1976) Computer recognition of roads from satellite pictures. IEEE Trans Syst Man Cybern SMC-6:623–637

Bentabet L, Jodouin S, Ziou D, Vaillancourt J (2003) Road vectors update using SAR imagery: a snake-based method. IEEE Trans Geosci Remote Sens 41(8):1785–1803

Borghys D, Perneel C, Acheroy M (2000) A multivariate contour detector for high-resolution polarimetric SAR images. In: Proceedings of the 15th International Conference Pattern Recognition, vol 3, pp 646–651, 3–7 September 2000

Caltagirone F, Spera P, Gallon A, Manoni G, Bianchi L (2001) COSMO-Skymed: a dual use Earth observation constellation. In: Proceedings of the 2nd international workshop on satellite constellation and formation flying, pp 87–94

Canny J (November 1986) A computational approach to edge detection. IEEE Trans Pattern Anal Mach Intell PAMI-8(11):679–698

Chanussot J, Mauris G, Lambert P (May 1999) Fuzzy fusion techniques for linear features detection in multitemporal SAR images. IEEE Trans Geosci Remote Sens 37(3):2287–2297

Chesnaud C, Réfrégier P, Boulet V (November 1999) Statistical region snake-based segmentation adapted to different physical noise models. IEEE Trans Pattern Anal Mach Intell 21(11):1145–1157

Dell'Acqua F, Gamba P (October 2001) Detection of urban structures in SAR images by robust fuzzy clustering algorithms: the example of street tracking. IEEE Trans Geosci Remote Sens 39(10):2287–2297

Dell'Acqua F, Gamba P (January 2003) Texture-based characterization of urban environments on satellite SAR images. IEEE Trans Geosci Remote Sens 41(1):153–159

Dell'Acqua F, Gamba P, Lisini G (2002) Extraction and fusion of street network from fine resolution SAR data. In: Proceedings of IGARSS, vol 1. Toronto, ON, Canada, pp 89–91, June 2002

Dell'Acqua F, Gamba P, Lisini G (2003). Road map extraction by multiple detectors in fine spatial resolution SAR data. Can J Remote Sens 29(4):481–490

Dell'Acqua F, Gamba P, Lisini G (2005) Road extraction aided by adaptive directional filtering and template matching. In: Proceedings of the third GRSS/ISPRS joint workshop on remote sensing over urban areas (URBAN 2005), Tempe, AZ, 14–16 March 2005 (on CD-ROM)

Dell'Acqua F, Gamba P, Trianni G (March 2006) Semi-automatic choice of scale-dependent features for satellite SAR image classification. Pattern Recognit Lett 27(4):244

Dell'Acqua F, Gamba P, Lisini G (2008) Rapid mapping of high-resolution SAR scenes. ISPRS J Photogramm Remote Sens, doi:10.1016/j.isprsjprs.2008.09.006

Dell'Acqua F, Lisini G, Gamba P (2009) Experiences in optical and SAR imagery analysis for damage assessment in the Wuhan, May 2008 earthquake. In: Proceedings of IGARSS 2009, Cape Town, South Africa, 13–17 July 2009

Dekker RJ (September 2003) Texture analysis and classification of ERS SAR images for map updating of urban areas in the Netherlands. IEEE Trans Geosci Remote Sens 41(9):1950–1958

Duskunovic I, Heene G, Philips W, Bruyland I (2000) Urban area selection in SAR imagery using a new speckle reduction technique and Markov random field texture classification. In: Proceedings of IGARSS, vol 2, pp 636–638, July 2000

Fischler MA, Tenenbaum JM, Wolf HC (1981) Detection of roads and linear structures in low resolution aerial imagery using a multisource knowledge integration technique. Comput Graph Image Process 15(3):201–223

Gamba P, Houshmand B (1999) Three-dimensional road network by fusion of polarimetric and interferometric SAR data. In: Proceedings of IGARSS099, vol 1, pp 302–304

Gamba P, Dell'Acqua F, Lisini G (2007) Raster to vector in 2D urban data. In: Proceedings of joint urban remote sensing event 2007, Paris, France, 13–15 April (on CD-ROM)

GEOEye Imagery Sources. http://www.geoeye.com/CorpSite/products/imagery-sources/Default.aspx#ikonos

Gouinaud C, Tupin F (1996) Potential and use of radar images for characterization and detection of urban areas. In: Proceedings of IGARSS, vol 1. Lincoln, NE, pp 474–476, May 1996

Hall O, Falorni G, Bras RL (2005) Characterization and quantification of data voids in the shuttle Radar topography mission data, IEEE Geosci Remote Sens Lett 2(2):177–181

He C, Xia G-S, Sun H (2006) An adaptive and iterative method of urban area extraction from SAR images. IEEE Geosci Remote Sens Lett 3(4):504–507

Heremans R, Willekens A, Borghys D, Verbeeck B, Valckenborgh J, Acheroy M, Perneel C (June 2005) Automatic detection of flooded areas on ENVISAT/ASAR images using an object-oriented classification technique and an active contour algorithm. In: Proceedings of the 31st international symposium on remote sensing of environment. Saint Petersburg, Russia, pp 20–24. http://www.isprs.org/publications/related/ISRSE/html/papers/219.pdf

Hess L, Melack J, Simonett D (1990) Radar detection of flooding areas beneath the forest canopy: a review. Int J Remote Sens 11(5):1313–1325

Horritt M, Mason D, Cobby D, Davenport I, Bates P (2003) Waterline mapping in flooded vegetation from airborne SAR imagery. Remote Sens Environ 85:271–281

Jeon B, Jang J, Hong K (1999) Road detection in spaceborne SAR images based on ridge extraction. In: Proceedings of ICIP, vol. 2. Kobe, Japan, pp 735–739

Jeon B-K, Jang J-H, Hong K-S (January 2002) Road detection in spaceborne SAR images using a genetic algorithm. IEEE Trans Geosci Remote Sens 40(1):22–29

Kurosu T, Fujita M, Chiba K (1995) Monitoring of rice crop growth from space using the ERS-1 C-band SAR. IEEE Trans Geosci Remote Sens 33(4):1092–1096

Landsat Legacy Project Website. http://library01.gsfc.nasa.gov/landsat/

NASA Jet Propulsion Laboratory: Missions. SEASAT. http://jpl.nasa.gov/missions/missiondetails.cfm?mission=Seasat

Lisini G, Tison C, Tupin F, Gamba P (2006) Feature fusion to improve road network extraction in high-resolution SAR images. IEEE Geosci Remote Sens Lett 3(2):217–221

McKeown DM, Denlinger L (1988) Cooperative methods for road tracking in aerial imagery. In: Proceedings of CVPR, Ann Arbor, MI, pp 662–672

Mena JB (December 2003) State of the art on automatic road extraction for GIS update: a novel classification. Pattern Recognit Lett 24(16):3037–3058

Negri M, Gamba P, Lisini G, Tupin F (2006) Junction-aware extraction and regularization of urban road networks in high-resolution SAR images. IEEE Trans Geosci Remote Sens 44(10):2962–2971

Pesaresi M, Gerhardinger A, Kayitakire F (2007) Monitoring settlement dynamics by anisotropic textural analysis by panchromatic VHR data. In: Proceedings of joint urban remote sensing event 2007, Paris, 11–13 April 2007 (on CD-ROM)

Service Régional de Traitement d'Image et de Télédétection (SERTIT). http://sertit.u-strasbg.fr/

Soille P, Pesaresi M (2002) Advances in mathematical morphology applied to geoscience and remote sensing. IEEE Trans Geosci Remote Sens 40(9):2042–2055

Stilla U, Soergel U, Thoennessen U (2003) Potential and limits of InSAR data for building reconstruction in built-up areas. ISPRS J Photogramm Remote Sens 58(1–2):113–123

The International Charter – Space and Major Disasters. http://www.disasterscharter.org/

Tison C, Nicolas JM, Tupin F, Maitre H (October 2004) A new statistical model for Markovian classification of urban areas in high-resolution SAR images. IEEE Trans Geosci Remote Sens 42(10):2046–2057

Treitz PM, Rotunno OF, Howarth PJ, Soulis ED (1996) Textural processing of multi-polarization SAR for agricultural crop classification. In: Proceedings of IGARSS'96, pp 1986–1988

Tupin F, Maitre H, Mangin J-F, Nicolas J-M, Pechersky E (March 1998) Detection of linear features in SAR images: application to road network extraction. IEEE Trans Geosci Remote Sens 36(2):434–453

Tupin F, Houshmand B, Datcu M (2002) Road detection in dense urban areas using SAR imagery and the usefulness of multiple views. IEEE Trans Geosci Remote Sens 40(11):2405–2414

Ulaby FT, Kouyate F, Brisco B, Williams THL (March 1986) Textural information in SAR images. IEEE Trans Geosci Remote Sens GE-24(2):235–245. ISSN: 0196-2892. Digital Object Identifier: 10.1109/TGRS.1986.289643

UNOSAT is the UN Institute for Training and Research (UNITAR) Operational Satellite Applications Programme. http://unosat.web.cern.ch/unosat/

Werninghaus R, Balzer W, Buckreuss St, Mittermayer J, Mühlbauer P (2004) The TerraSAR-X mission. EUSAR, Ulm, Germany

Wessel B (2004) Context-supported road extraction from SAR imagery: transition from rural to built-up areas. In: Proceedings of the EUSAR, Ulm, Germany, pp 399–402, May 2004

Yu S, Berthod M, Giraudon G (July 1999) Toward robust analysis of satellite images using map information-application to urban area detection. IEEE Trans Geosci Remote Sens 37(4): 1925–1939

http://www.springer.com/978-90-481-3750-3

Radar Remote Sensing of Urban Areas
Soergel, U. (Ed.)
2010, XVI, 278 p. 120 illus., Hardcover
ISBN: 978-90-481-3750-3